

SUPPORTING INFORMATION:

Novel synthesis of platinum complexes and their intracellular delivery to tumor cells by means of magnetic nanoparticles

Alessandra Quarta,^{a} Manuel Amorín,^b María José Aldegunde,^b Laura Blasi,^c Andrea Ragusa,^{a,d} Simone Nitti,^e Giammarino Pugliese,^e Giuseppe Gigli,^{a,f} Juan R. Granja,^{b*} Teresa Pellegrino^{e*}*

^a CNR NANOTEC – Institute of Nanotechnology, c/o Campus Ecotekne, via Monteroni, 73100, Lecce, Italy

^b Centro Singular de Investigación en Química Biolóxica e Materiais Moleculares (CIQUS) and Departamento de Química Orgánica, Universidade de Santiago de Compostela, 15782 Santiago de Compostela, Spain

^c CNR, Institute for Microelectronics and Microsystems, Via Monteroni, Lecce, 73100, Italy

^d Dipartimento di Scienze e Tecnologie Biologiche e Ambientali, Università del Salento, Campus Ecotekne, via Monteroni, 73100, Lecce, Italy

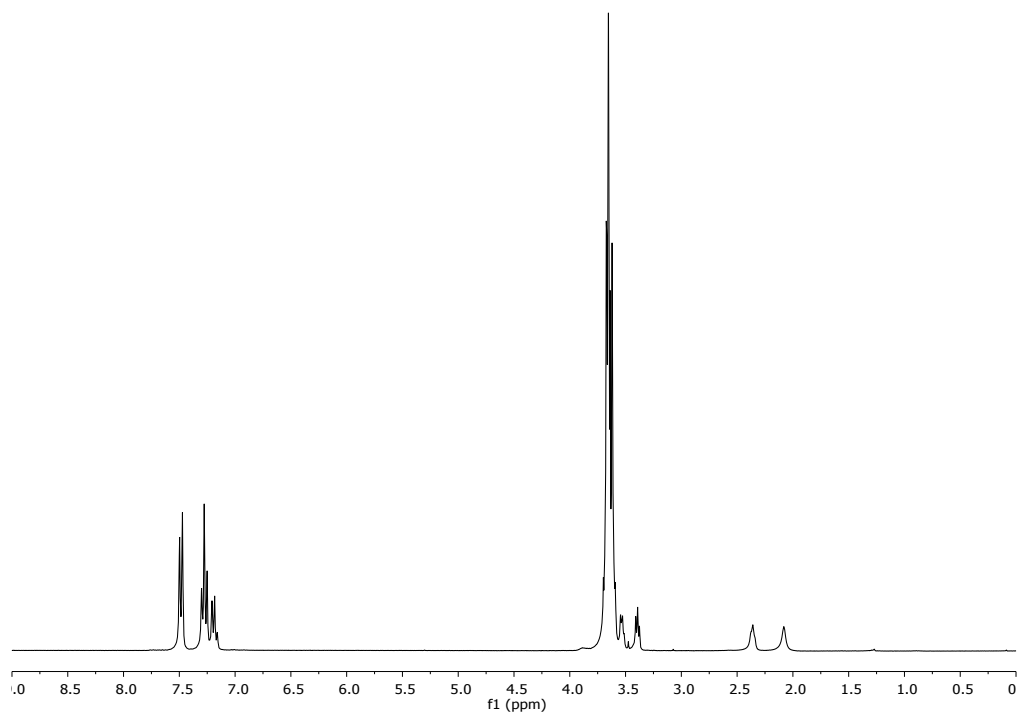
^e Istituto Italiano di Tecnologia, via Morego 30, 16163, Genova, Italy

^f Dipartimento di Matematica e Fisica E. De Giorgi, Università del Salento, Campus Ecotekne, via Monteroni, 73100, Lecce, Italy

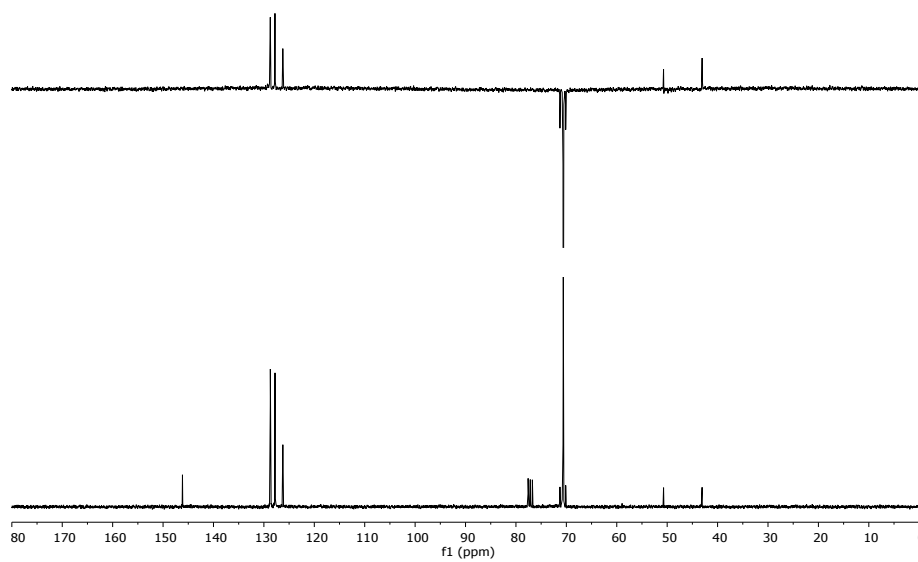
Nuclear Magnetic Resonance Spectra

- Azido-PEG-amine-Trt.

^1H NMR (300 MHz, CDCl_3):

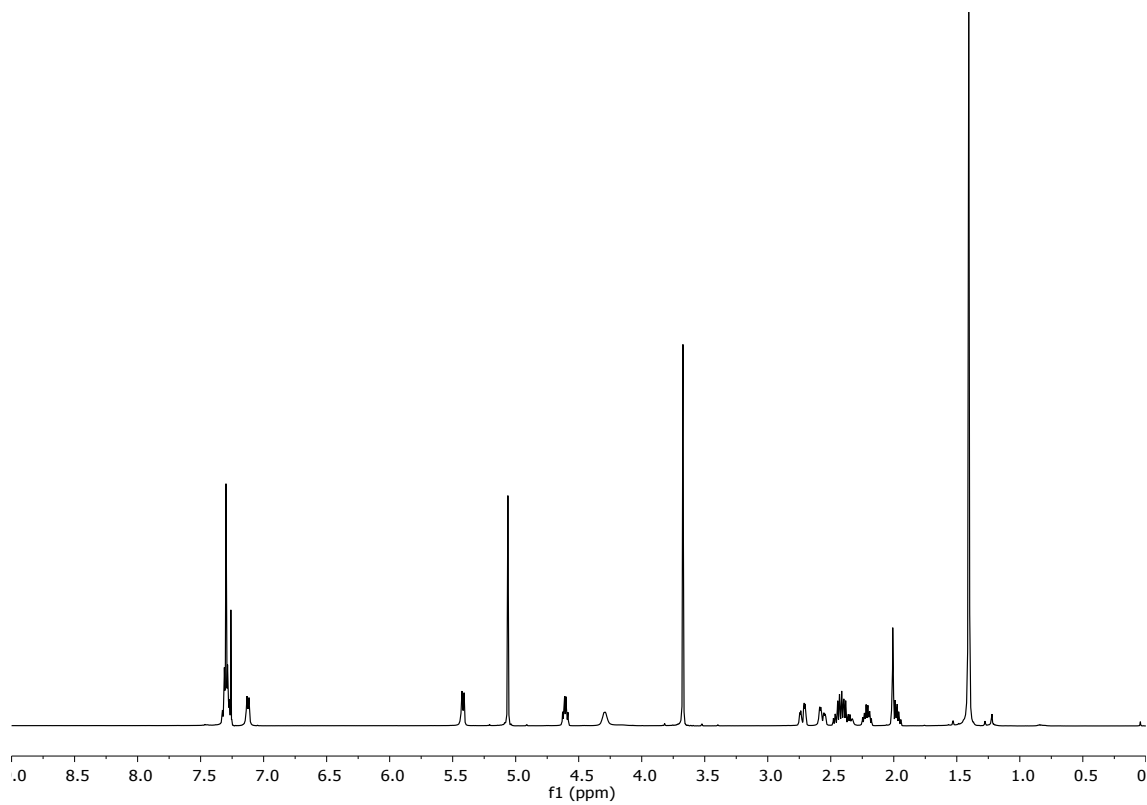


^{13}C NMR (75 MHz, CDCl_3):

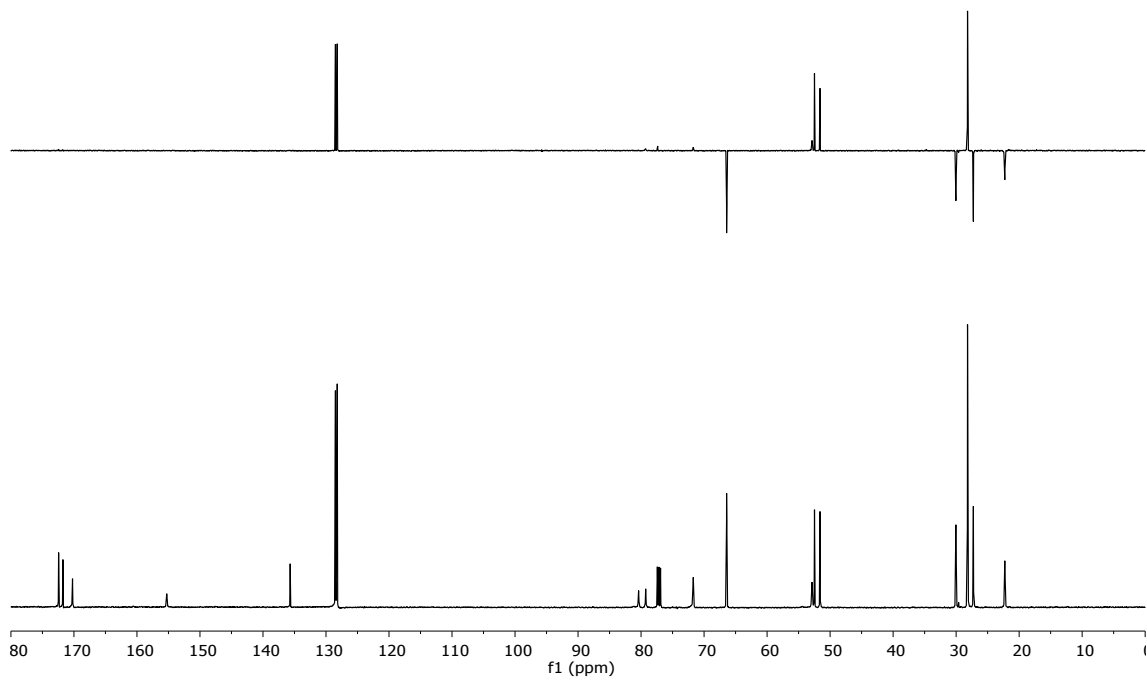


- **Boc-L-Pra-L-Glu(OBn)-OMe.**

^1H NMR (500 MHz, CDCl_3):

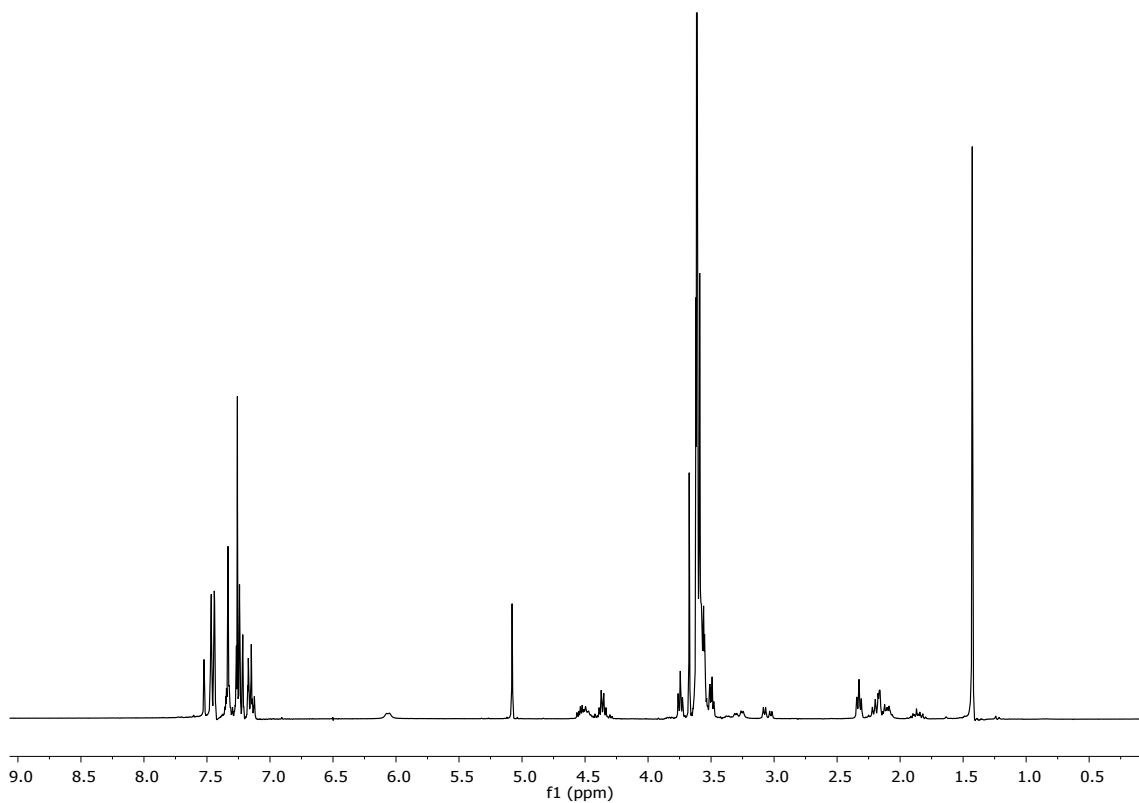


^{13}C NMR (125 MHz, CDCl_3):

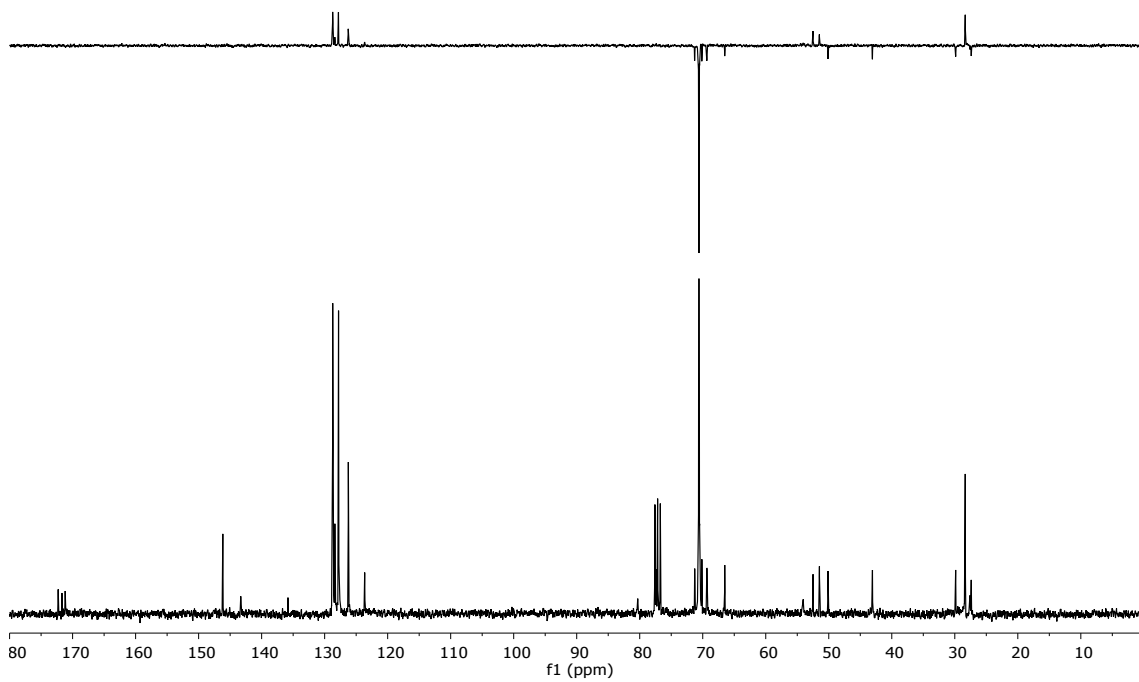


- **Boc-L-Ala(Triazol-PEG-amine-Trt)-L-Glu(OBn)-OMe.**

^1H NMR (300 MHz, CDCl_3):

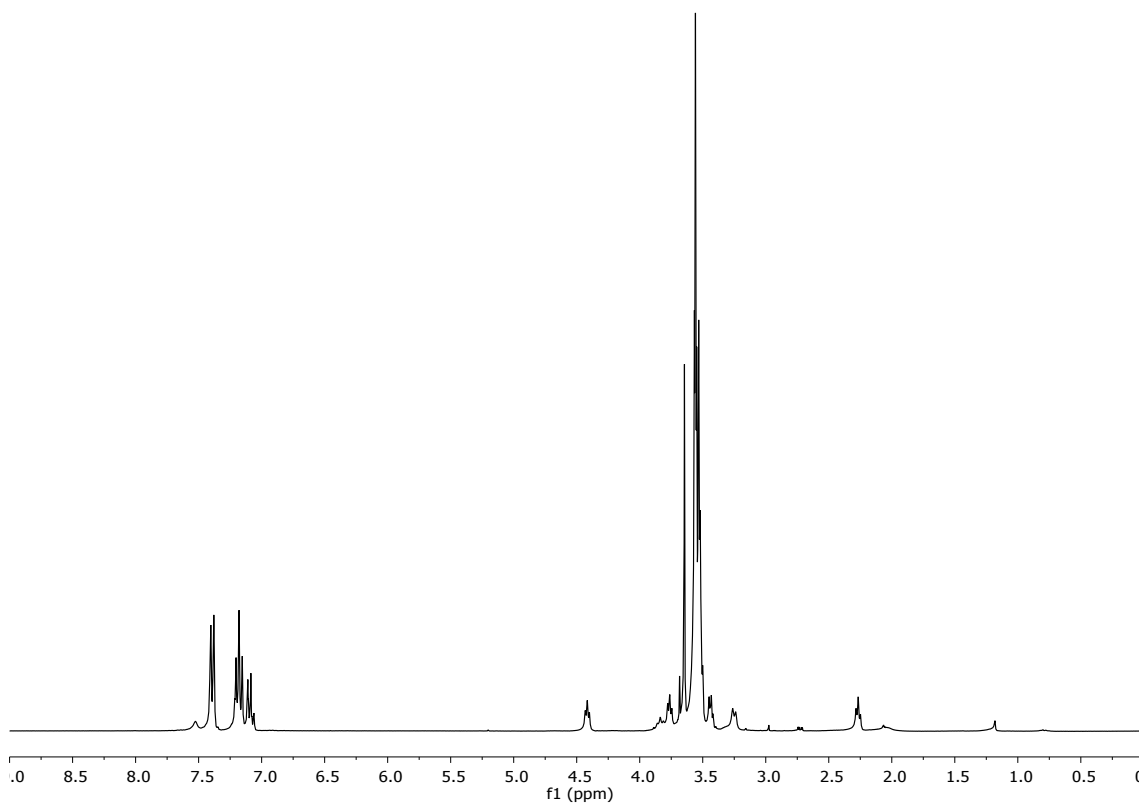


^{13}C NMR (75 MHz, CDCl_3):

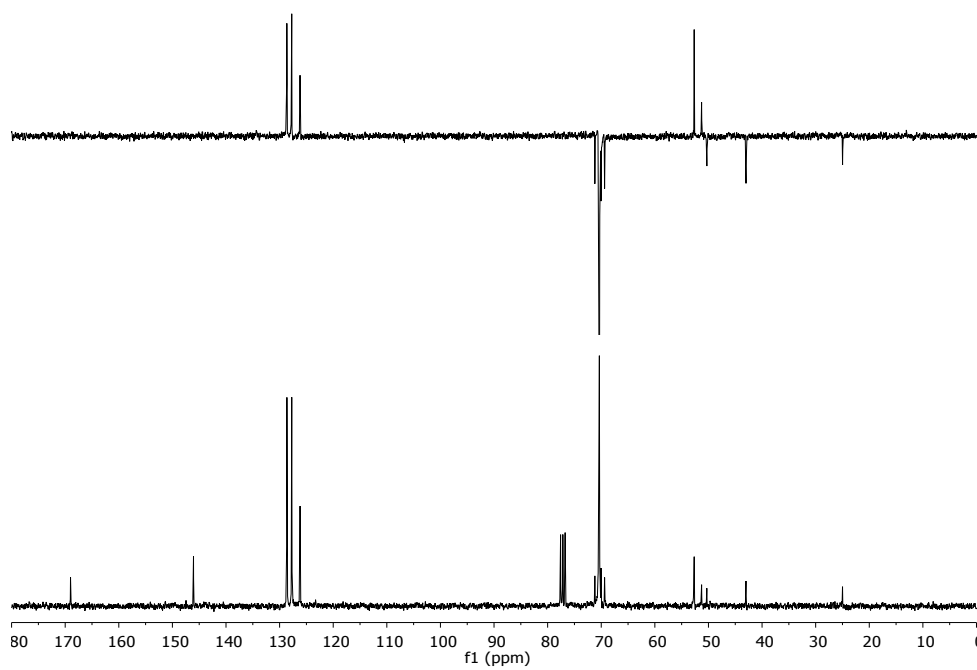


- **Tr-PEG-Mal-OMe**

^1H NMR (300 MHz, CDCl_3):

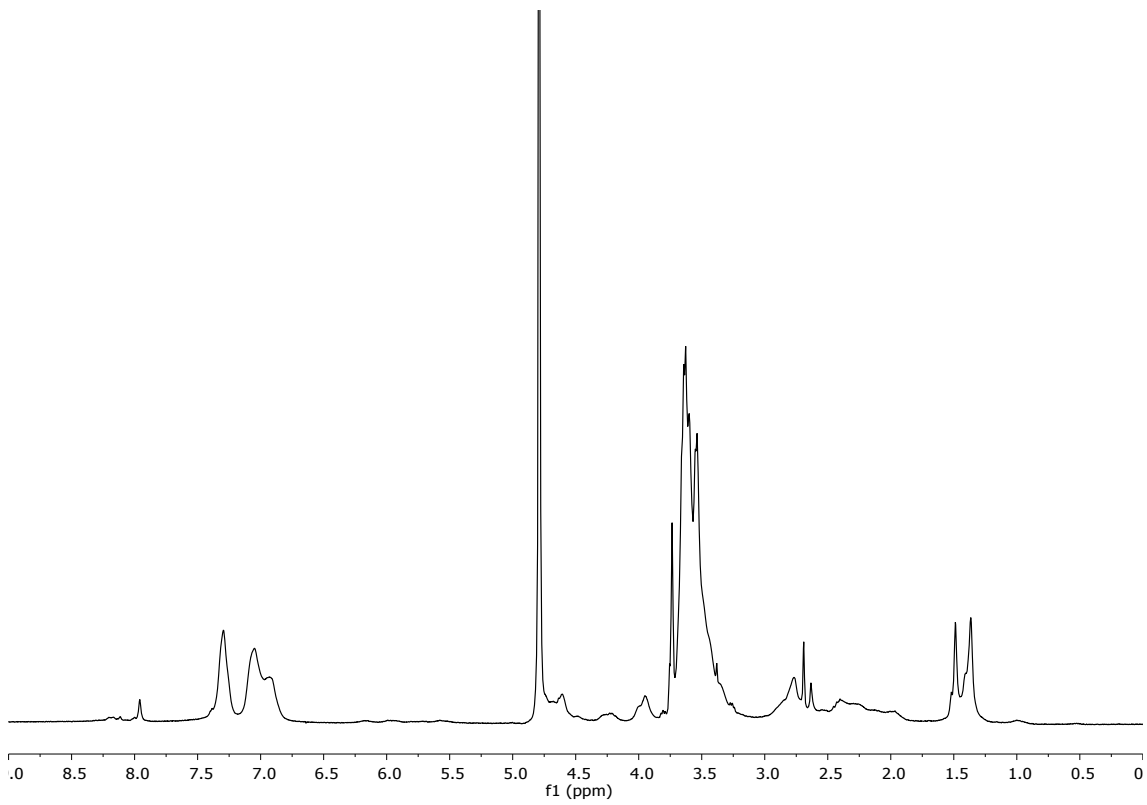


^{13}C NMR (75 MHz, CDCl_3):



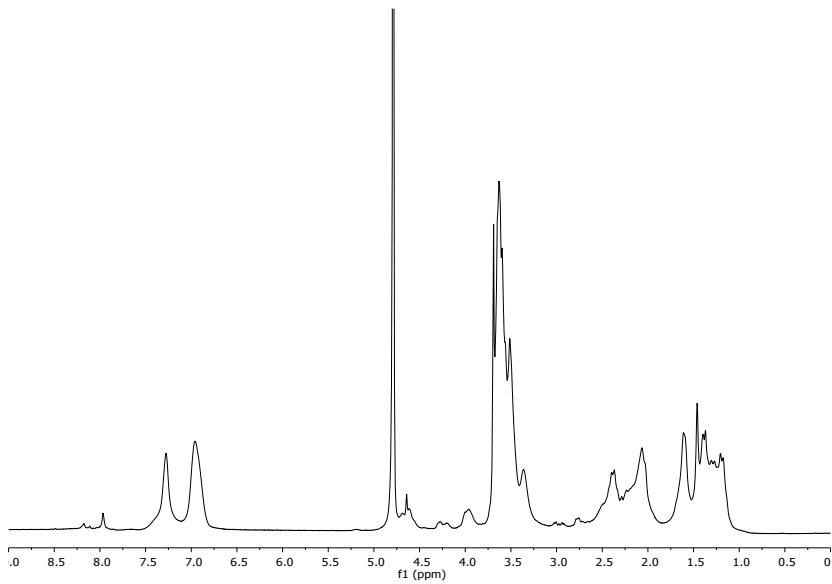
- **Tr-PEG-Glu-Pt-EDA.**

^1H NMR (300 MHz, D_2O):



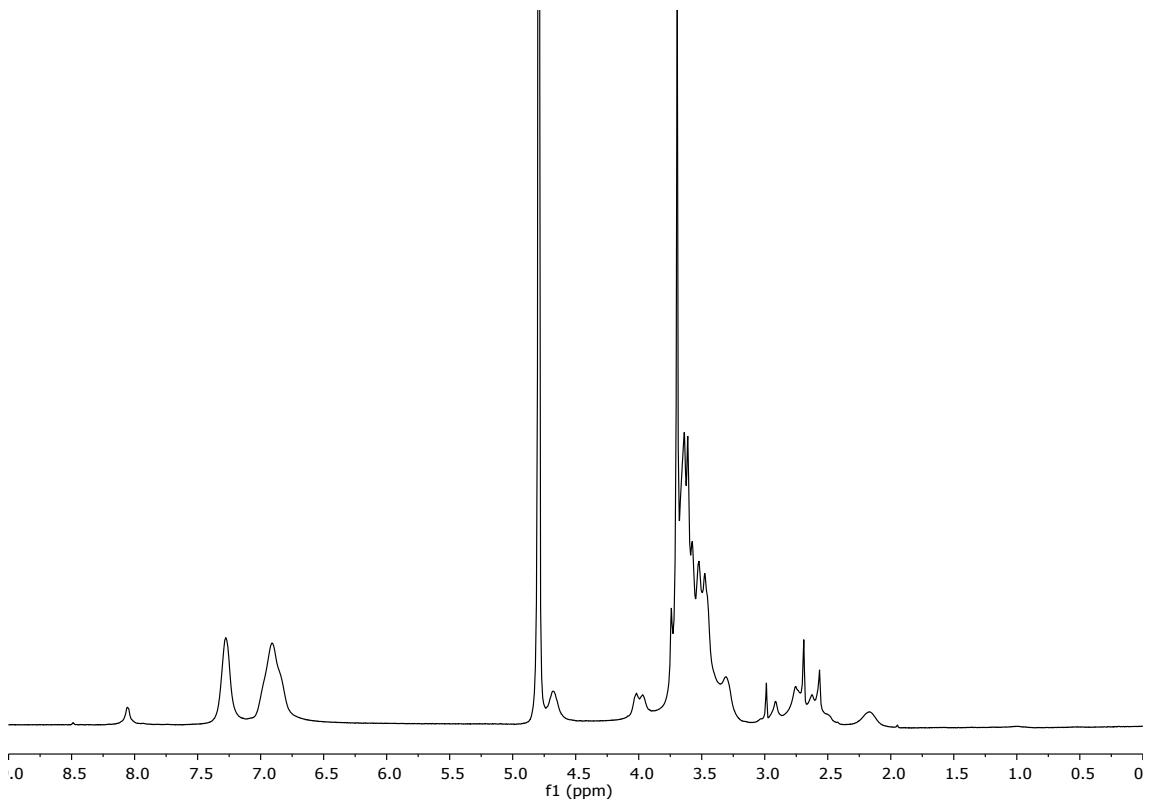
- **Tr-PEG-Glu-Pt-DACH).**

¹H NMR (300 MHz, D₂O):



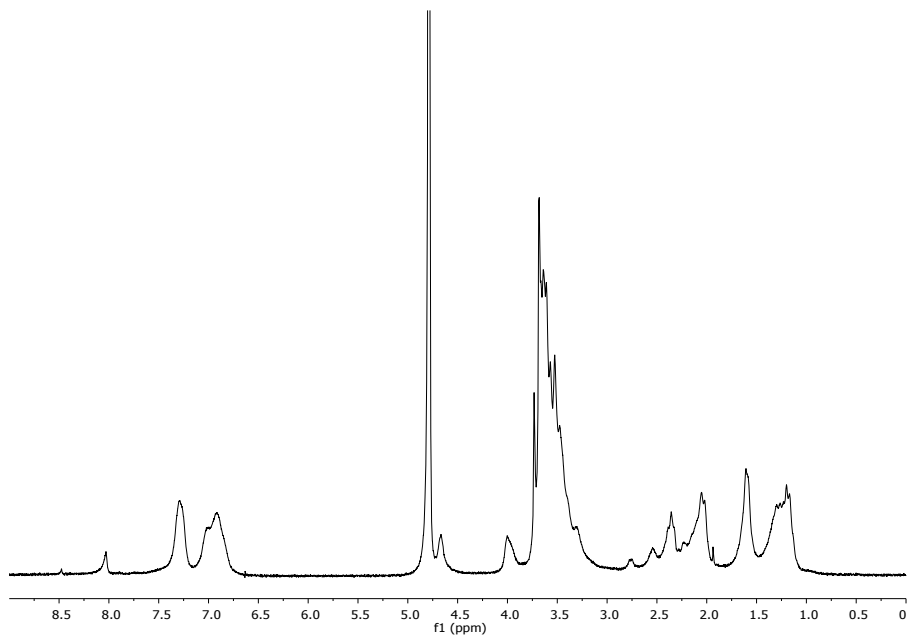
- **Tr-PEG-Mal-Pt-EDA.**

¹H NMR (300 MHz, D₂O):



- Tr-PEG-Mal-Pt-DACH.

^1H NMR (300 MHz, D_2O):



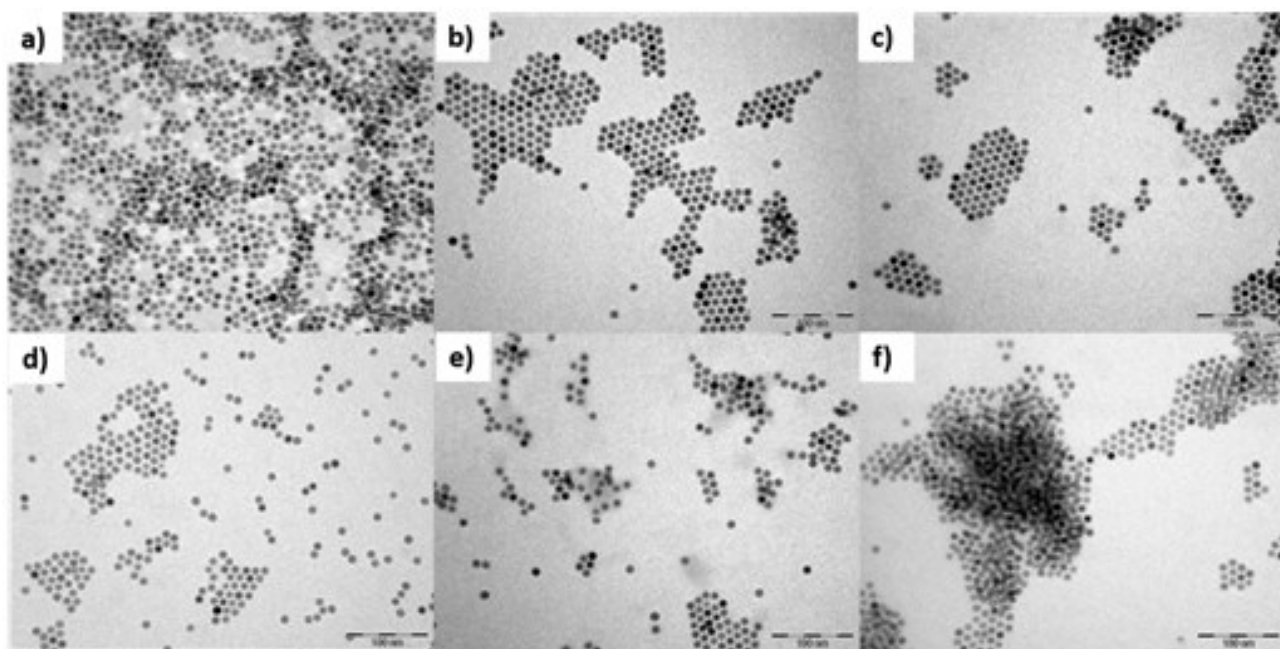


Figure 1SI. TEM images of MNP a) soon after the synthesis in CHCl_3 , b) post PEG functionalization, c-f) conjugated to, **PEG-Mal-Pt-EDA**, **PEG-Mal-Pt-DACH**, **PEG-Glu-Pt-EDA** and **PEG-Glu-Pt-DACH** respectively.

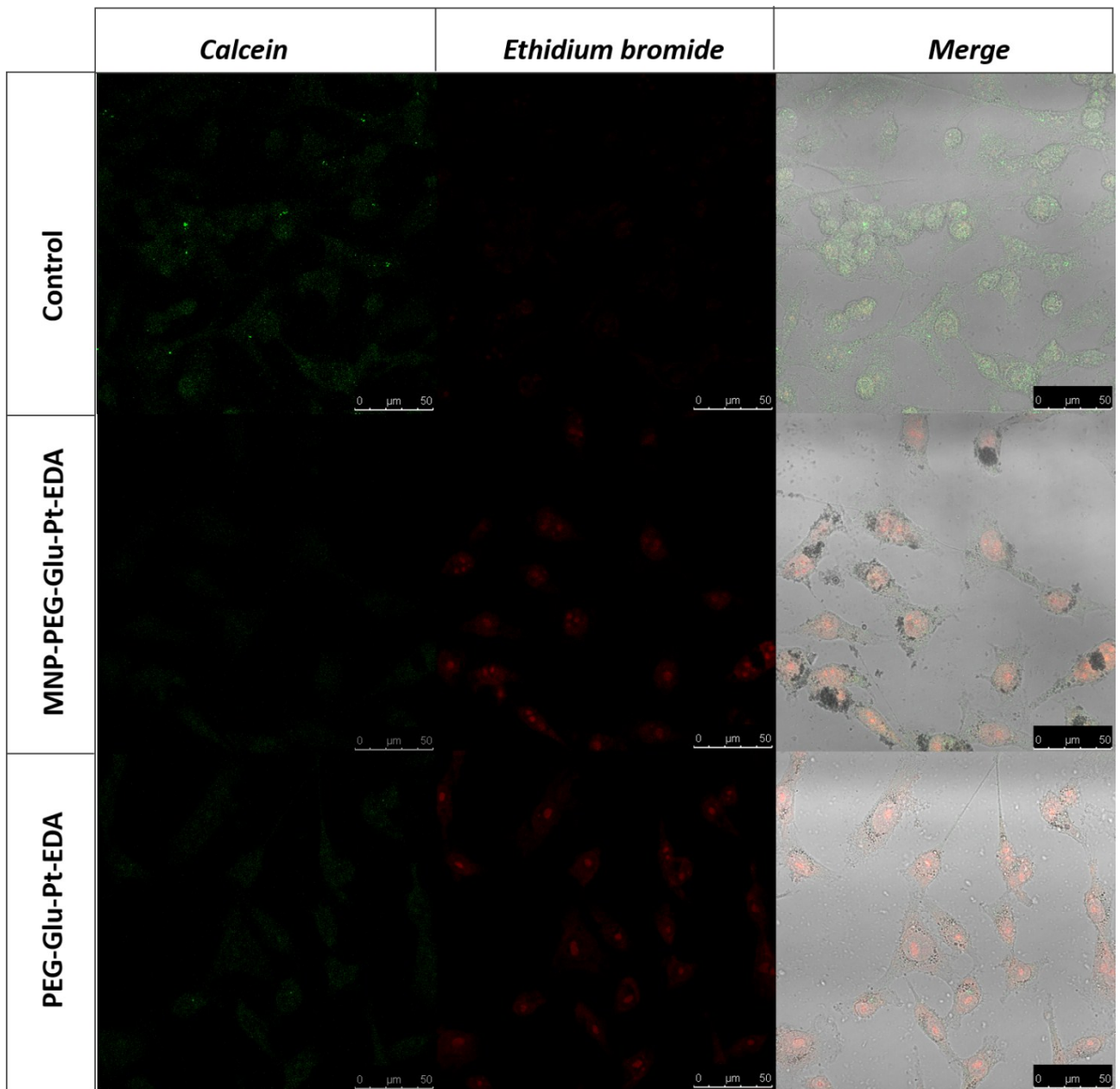


Figure 2SI. A live-dead assay, which was performed with MDA-MB-231 cells incubated with either a MNP-PEG-Glu-Pt-EDA conjugate or a free PEG-Glu-Pt-EDA complex for 24 h.

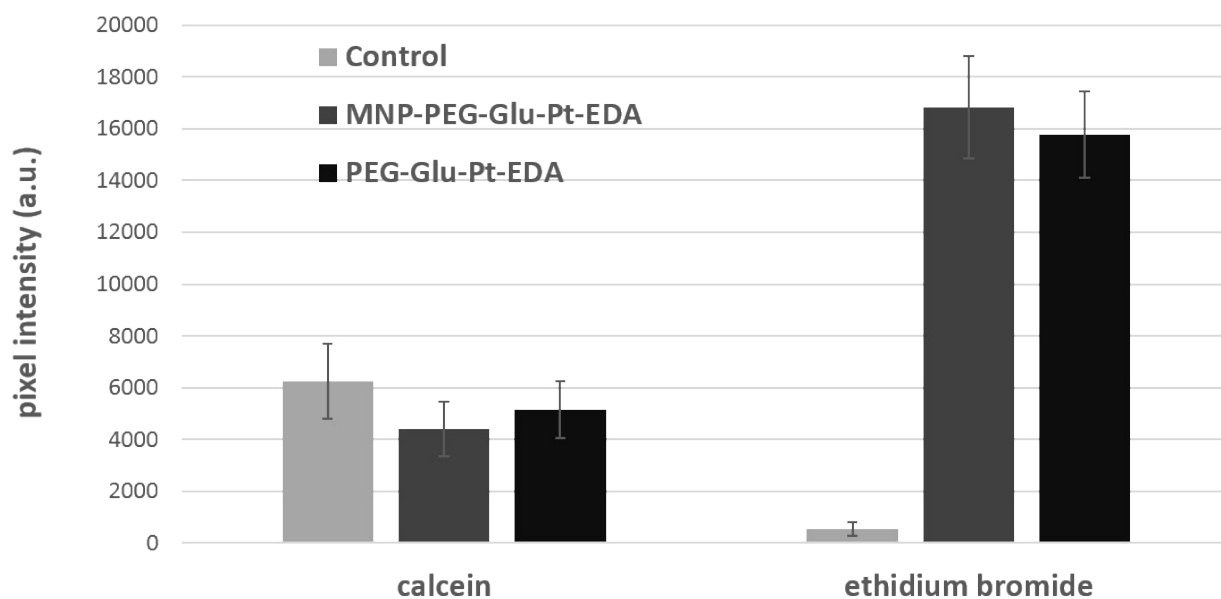


Figure 3SI. Quantitative analysis performed on fluorescent pixels of confocal images of MDA-MB231 cells administered with either free **PEG-Glu-Pt-EDA** or **MNP-PEG-Glu-Pt-EDA** and then stained with live/dead assay. Analysis was carried out on both calcein and ethidium bromide fluorescent channels. Control cells were included in the analysis and values of pixel intensities for each fluorescent channel are mean \pm SD (n = 50).

	24 h		48 h	
	<i>caspase 3 (% activity)</i>	<i>s.d.</i>	<i>caspase 3 (% activity)</i>	<i>s.d.</i>
IGROV-1				
PEG-Mal-Pt-EDA	42,1	3,21	43,7	8,1
PEG-Mal-Pt-DACH	48,7	5,48	44,0	5,7
PEG-Glu-Pt-EDA	51,9	8,2	51,3	6,2
PEG-Glu-Pt-DACH	50,4	2,46	47,9	5,3
MNP-PEG-Mal-Pt-EDA	67,5	3,48	68,3	8,5
MNP-PEG-Mal-Pt-DACH	70,7	5,71	68,0	7,6
MNP-PEG-Glu-Pt-EDA	73,9	2,13	70,9	4,8
MNP-PEG-Glu-Pt-DACH	73,5	6,55	72,6	5,7
MNP-PEG	26,7	2,2	29,2	4,3
MDA-MB-231				
PEG-Mal-Pt-EDA	28,1	5,32	31,8	3,3
PEG-Mal-Pt-DACH	30,9	2,5	26,1	4,4
PEG-Glu-Pt-EDA	32,1	3,72	33,3	4,9
PEG-Glu-Pt-DACH	27,3	4,7	36,4	5,2
MNP-PEG-Mal-Pt-EDA	61,0	2,38	53,7	5,8
MNP-PEG-Mal-Pt-DACH	60,8	6,74	54,5	3,3
MNP-PEG-Glu-Pt-EDA	64,4	4,26	54,6	3,7
MNP-PEG-Glu-Pt-DACH	63,5	3,1	56,1	4,3
MNP-PEG	17,3	2,8	16,0	2,6

Table 1SI. Results of the caspase-3 assay performed with IGROV-1 cells and MDA-MB-231 cells incubated with the four MNP-Pt conjugates, the free Pt complexes, and MNP-PEG for 24 and 48 h.

The data are reported as a percentage of the fluorescence intensity of each sample with respect to the control cells and represent the average \pm SD of three independent experiments.

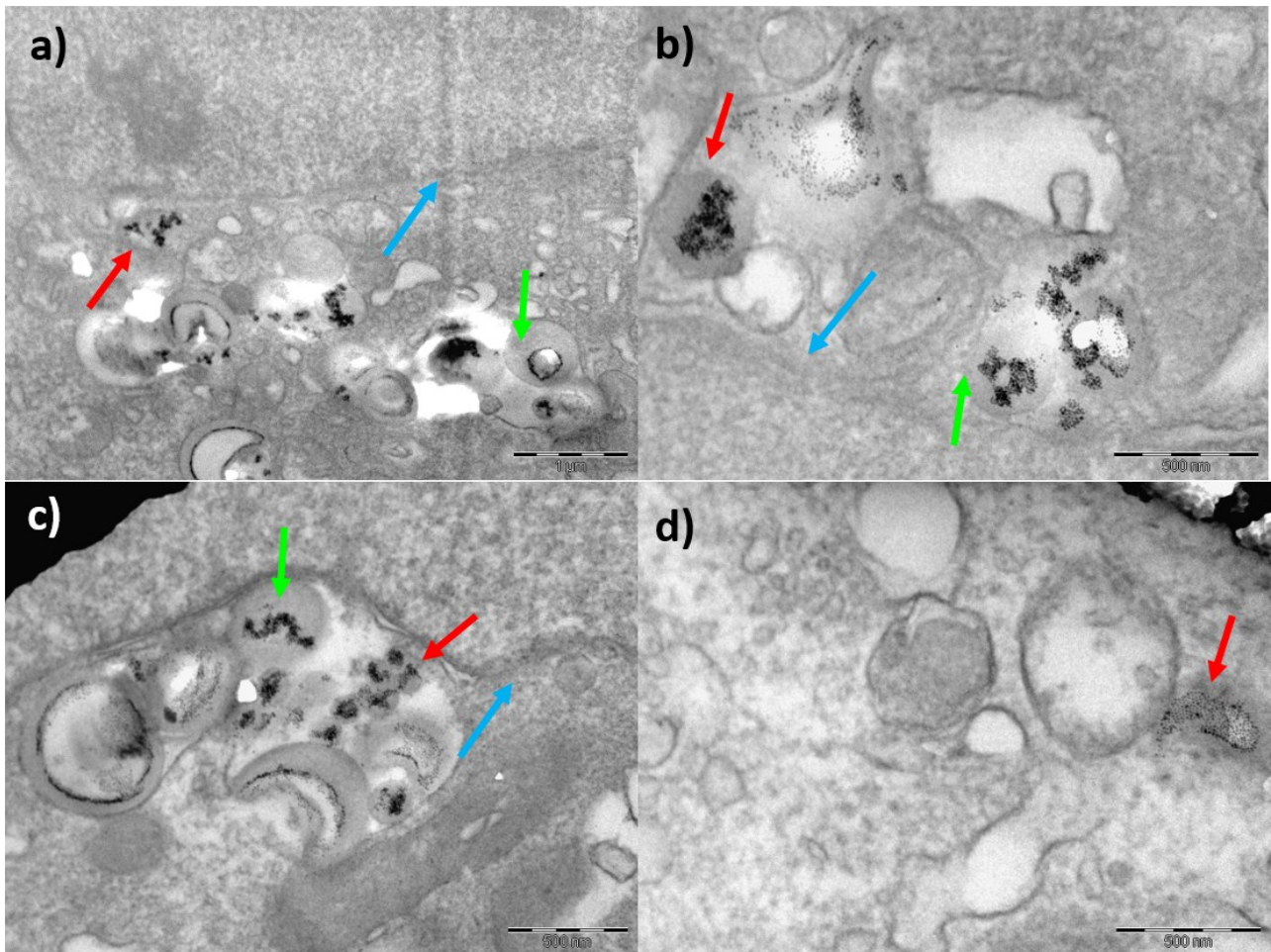


Figure 4SI. TEM images of IGROV-1 cells incubated for 24 h with **MNP-PEG-Glu-Pt-EDA**. Red arrows indicate endolysosomes containing nanoparticles; green arrows indicate swollen vesicles containing nanoparticles. Blue arrows point to the nuclear membrane.

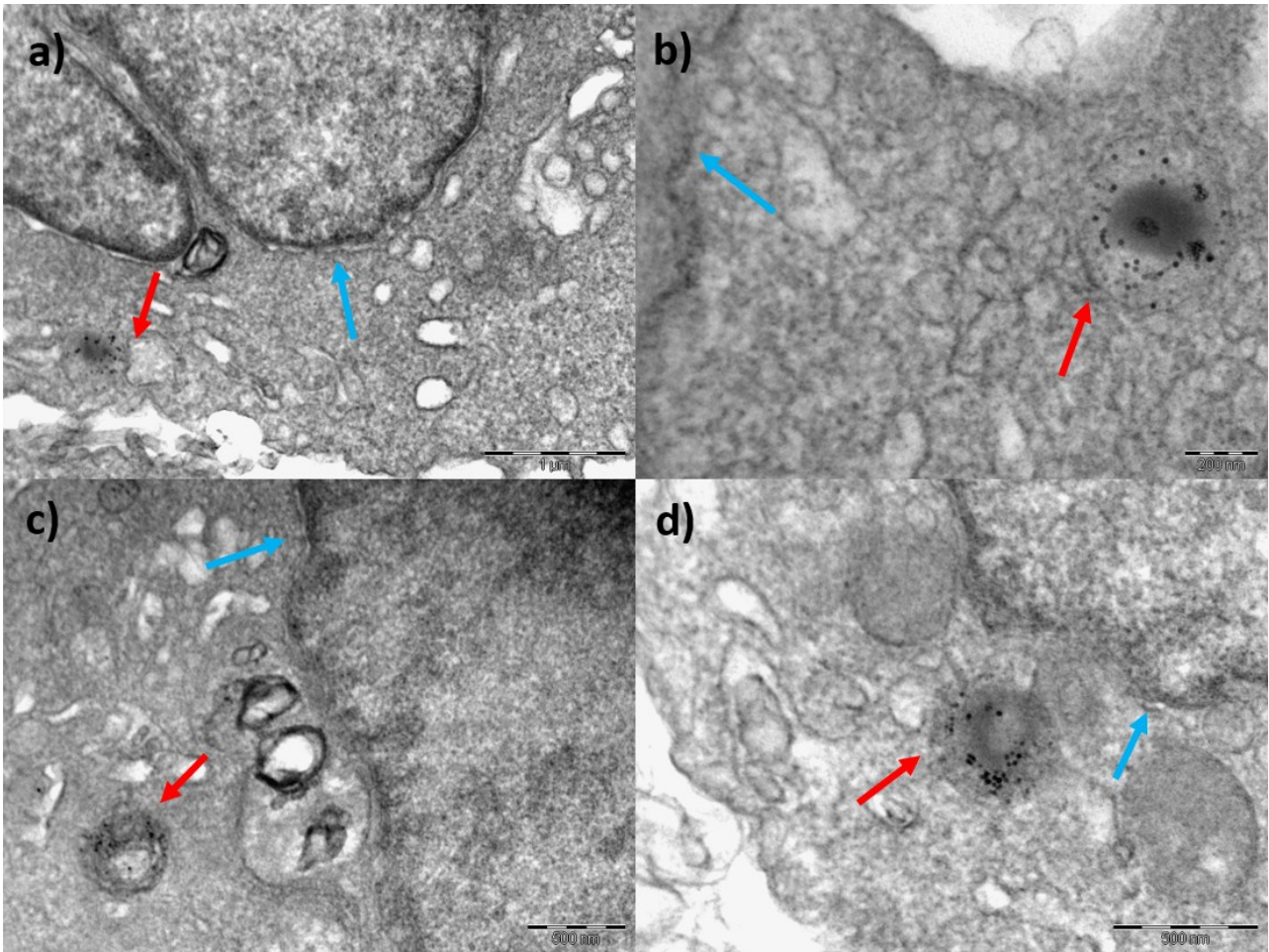


Figure 5SI. TEM images of IGROV-1 cells incubated for 24 h with **MNP-PEG**. Red arrows indicate endolysosomes containing nanoparticles, while blue arrows point to the nuclear membrane.

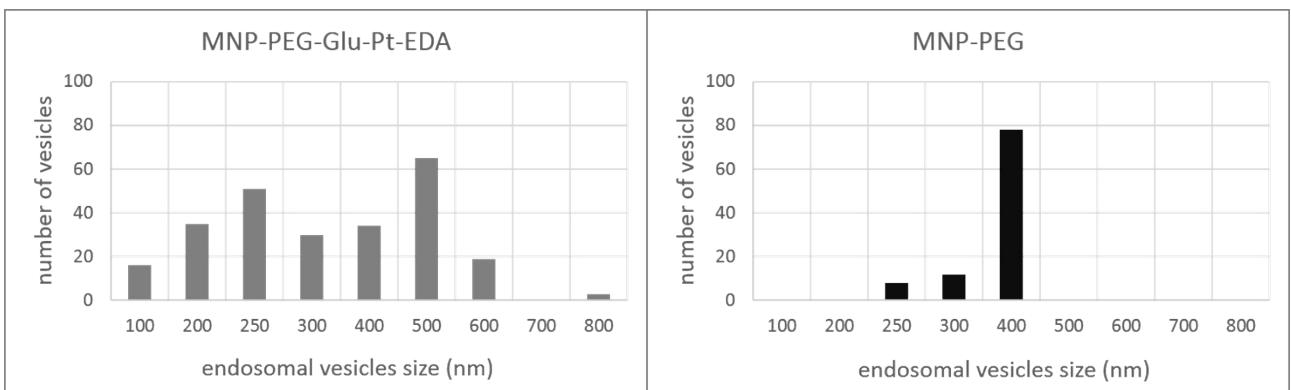


Figure 6SI. Analysis of the size distribution of endosomal vesicles performed on TEM images of IGROV-1 cells incubated for 24 h with either **MNP-PEG-Glu-Pt-EDA** or **MNP-PEG**.

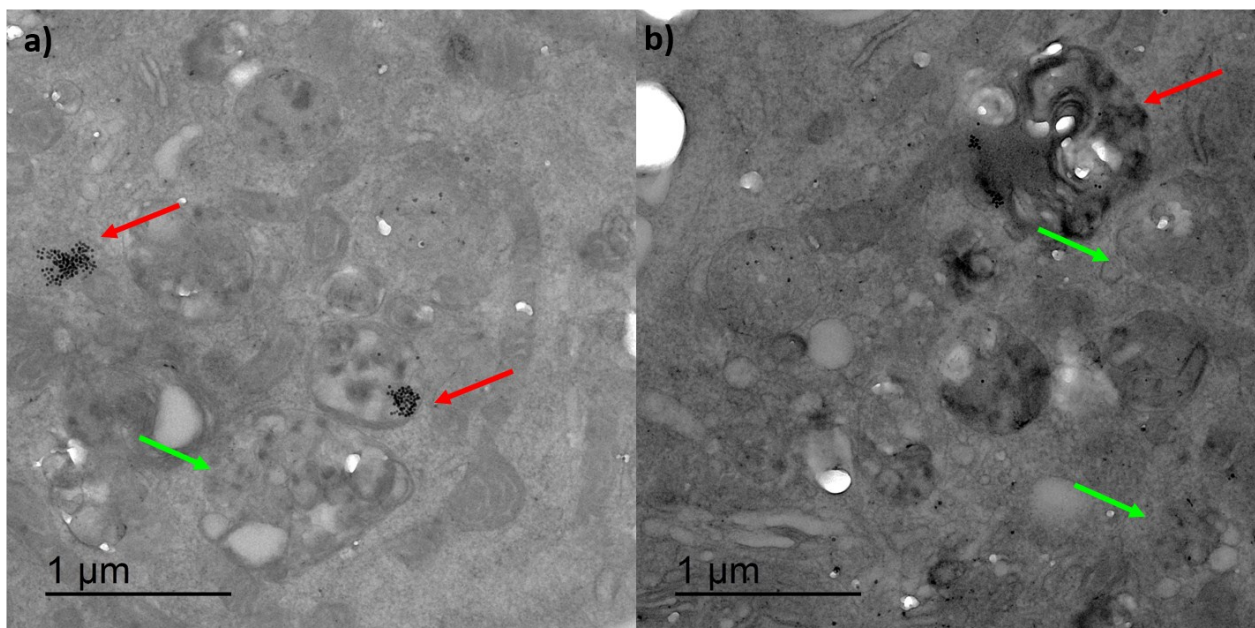


Figure 7SI. TEM images of IGROV-1 cells incubated continuously with **MNP-PEG-Glu-Pt-EDA** for 1 h, and then kept in culture for additional 96 h. Red arrows indicate endolysosomes containing nanoparticles, while green arrows point to the vacuoles.

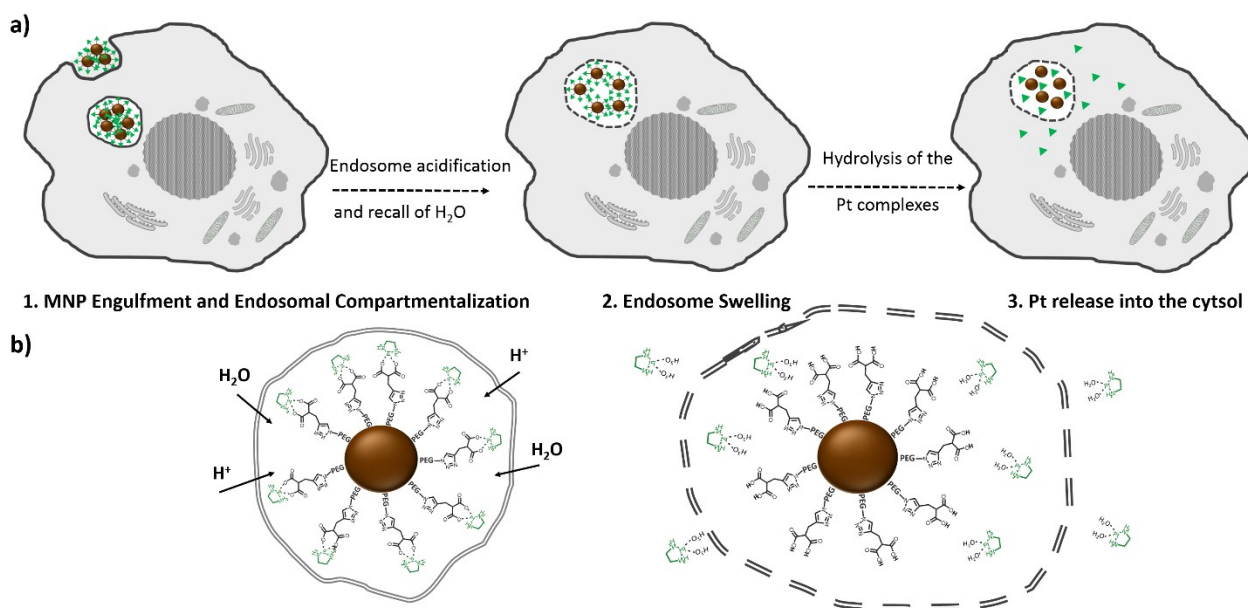


Figure 8SI. a) Sketch showing the proposed mechanism of Pt release from the Pt-MNP conjugates. 1. The nanoparticles are engulfed and sequestered into the endosomes. 2. Then, endosome acidification enhanced by the triazole moiety induces water recall with consequent swelling. 3. The Pt complex undergoes hydrolysis allowing the release of the active species and the escape from the endosome to the cytosol. b) Magnification of the hydrolysis mechanism and release of the active species. The drawings are not to scale.